

# Magneto-mineralogical characterization and manifestations of magnetic fabrics from the gneissic rocks and associated intrusive bodies in and around Bankura and Purulia districts, West Bengal, India

Saurodeep Chatterjee<sup>1,\*</sup>, Supriya Mondal<sup>1</sup>, Pratik Roy<sup>1,2</sup>, Debesh Gain<sup>1</sup> and Amitava Bhattacharya<sup>1,3</sup>

<sup>1</sup>Department of Geological Sciences, Jadavpur University, Kolkata 700 032, India

<sup>2</sup>National Thermal Power Corporation (NTPC) Limited, Noida 201 301, India

<sup>3</sup>Geological Survey of India, Central Headquarters, Kolkata 700 016, India

The present study aims to unravel the mineralogical, chemical and anisotropy of magnetic susceptibility (AMS) from gneissic rocks and associated pegmatitic bodies from Bankura–Purulia region, West Bengal (India). Petrographic studies were done to detect the textural relationship of minerals that contribute susceptibility with that of the silicates. The study of polished thin-sections under reflected light microscope showed the presence of titanomagnetite and magnetite as dominant magnetic minerals. More than one generation of magnetic minerals were found which are linked to different conditions of temperature and tectonics that prevailed during their oxidation. AMS studies depicted the overall nature of magnetic fabrics (and other related parameters like mean susceptibility, magnetic foliation, magnetic lineation, corrected degree of anisotropy, shape parameter) in the region. The susceptibility ellipsoids were dominantly oblate in the region as evident from the  $P_j-T_j$  plots. The absence of linear relationship between mean susceptibility and degrees of anisotropy proves that the fabrics are independent of bulk ferromagnetic susceptibility and controlled by deformational features. The equal area plots of the principal susceptibility axes and representation of maximum susceptibility axes in the rose diagram revealed parity between the field and magnetic fabrics thus pointing to a tectonic control of fabrics. Moreover, the pegmatitic bodies based on AMS parameters are found to have emplace syn-tectonic to basement deformation which impinged a linear feature (both in mesoscopic fabric and magnetic fabric) to the otherwise undeformed intrusive bodies.

**Keywords:** Atomic Absorption Spectrophotometry, Anisotropy of Magnetic Susceptibility, Fe–Ti-oxide, gneiss, pegmatites.

\*For correspondence. (e-mail: chatterjeesaurodeep@gmail.com)

EXPOSURES of the Chhotanagpur Gneissic Complex (CGC) in the Bankura and Purulia districts of West Bengal, India can be considered as type sections for varied geological and geophysical studies. Extensive studies have been done and are still being pursued in the fields of petrological, mineralogical and economic geology in this region. Such Precambrian terrains are extremely useful in studying the magnetic properties related to different geological events<sup>1</sup>. Determination of various stages of magnetic minerals (mainly titanomagnetite), corresponding to different temperatures will help predict the tectonic events that drive their formation. Despite these characteristics of rocks, under present consideration, the magneto-mineralogical characteristics and the nature of magnetic fabrics of rocks remain obscure. In the following sections the petrological and chemical nature, magneto-mineralogical characteristics and the nature of magnetic fabrics of rocks of the studied area in Bankura and Purulia districts are discussed. Further the orientations of principle magnetic susceptibility axes of the values of various anisotropy of magnetic susceptibility (AMS) parameters were analysed to correlate magnetic fabrics with that of tectonic fabrics of rock bodies within the region in the studied area.

## Geological features of the Chhotanagpur gneissic complex

The studied area belongs to the south-eastern part of Purulia district and areas near the boundary between Purulia and Bankura districts, West Bengal, under the Survey of India Toposheet No. 73 I/15. It is situated between lat. 23°25′–23°20′N and long. 86°45′–86°40′E (Figure 1). The area is around 1000 m above mean sea level (amsl) with NE–SW trending hills. The terrain is drained by the Dwarkeshwar river, which flows from NW

to SE. Several nalas (viz. Dangra nala, Adam nala) also drain the area. Because of the undulatory topography, the soil is gravelly in nature. There is a thin soil cover which contains high amount of iron with little organic matter giving a reddish tint to the soils of the studied area.

### Geological setting

The CGC located in the northern part of the East Indian Shield is composed of granulite–gneiss terrain largely containing granitic rocks with patchy occurrences of meta-pelites (khondalite, quartz-kyanite-garnet rock, quartz-sillimanite-corundum rock, etc.), quartzites, ortho- and para-amphibolites, calc-granulites and recrystallized limestones, gabbro-norite-anorthosite, pyroxene-granulite, charnockite, leptynite, alkali syenite, apatite-magnetite rocks, banded garnetiferous magnetite-ilmenite rocks, numerous pegmatites and pneumatolytic hydrothermal veins<sup>2</sup>. CGC suffered polyphase magmatism and metamorphism. Ghose<sup>3</sup> reported that in CGC the early phase granites were sodic varieties like tonalite and quartz-diorite, but the late phase granites were of potassic

varieties like porphyritic granites. The late phase basic magmatic activities (dolerite, gabbro, pyroxenite intrusives in the early stage and basaltic volcanics, i.e. Rajmahal traps in the much later stage) are also evident in CGC. The metamorphic rocks belonging to CGC mainly consist of granite gneiss, biotite granite gneiss, calc-granulites, ultrabasic, metabasic, meta-sediments including crystalline limestone, and garnetiferous sillimanite–biotite schist which contains minor Kyanite at some places<sup>2</sup>.

The rocks in the studied part of CGC (Figure 1) are medium to high grade metamorphosed with concordant and discordant intrusive bodies like dolerite and pegmatite<sup>4</sup>. Geochronologically, these rocks are assigned to two age groups,  $870 \pm 40$  Ma and  $810 \pm 40$  Ma, from the K–Ar dating of biotite from the porphyritic granitoid and muscovite from the leuco-granitoid<sup>5,6</sup>. Structurally, there occurs an overall E–W to NE–SW trend within the rocks of Paharpur and Gopalpur regions with northerly dips of the gneissic banding that happens to be the dominant field fabric within the basement granitoid gneisses of the CGC. The reason for this constant northerly dip in this particular region is attributed by earlier studies to the presence of isoclinal folds<sup>7–10</sup>. The present field studies and earlier observations<sup>5,6</sup> reveal that the nature of dominant field foliation is quite changed in the Dangra nala and Dwarkeshwar river area with ESE–WNW trend and low dips towards N and NNE. These formations are intruded by granitic rocks and at places by pegmatites (Figure 1). The pegmatite bodies possess elliptical outcrops. Although the rocks are massive, crude mineral lineations developed, trend the NW–SE with moderate plunges.

### Methodology

Oriented samples are of utmost importance for carrying out magnetic susceptibility and AMS<sup>11</sup> studies. Suitable locations were selected, from which 6–8 oriented cores (diameter of 2.54 cm and height of 2.2 cm) were drilled using a portable drilling machine<sup>12,13</sup>. Twenty five locations were selected for collection of oriented cores. Among 25 locations, 18 sites had suitable exposures for on-site drilling. From the remaining six sites, oriented block samples were collected and were further drilled to cores in the laboratory. Chemical analysis of rock samples was done mainly to determine the proportion of iron within the samples with an aim to detect the dominance of iron oxides within the studied rock samples. For chemical analysis by Atomic Absorption Spectrophotometry (AAS), samples from the field were crushed and ground to a size of 200 mesh using the ball mill and hammer mill in the metallurgical laboratory and were analysed in the AAS laboratory in the Centre for Bio-equivalence, Jadavpur University, Kolkata.

The magnetic studies were carried out in two steps: magnetic susceptibility measurement and AMS measurement.

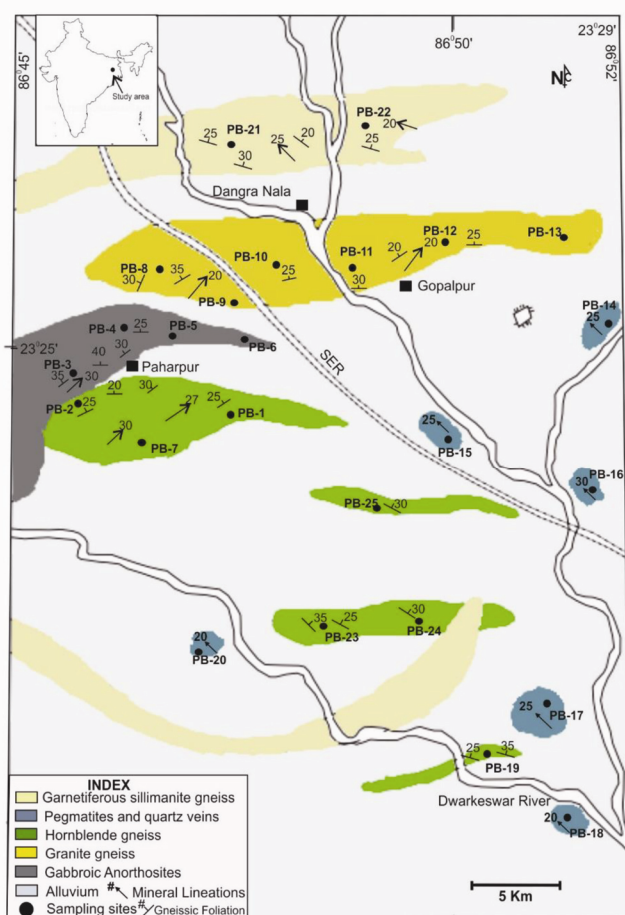


**Figure 1.** Generalized map of the study area showing rock types present and sampling sites.



**Figure 2.** Granite gneisses with compositional banding (right); Granite gneisses with porphyroblasts (left) at Paharpur region.

The AMS measurements yielded the magnitudes and directions of the three principal axes of susceptibility ellipsoid  $K_1$ ,  $K_2$  and  $K_3$  ( $K_1 \geq K_2 \geq K_3$ ). The magnitudes of  $K_1$ ,  $K_2$  and  $K_3$  determine mean susceptibility, magnetic foliation, magnetic lineation and degree of anisotropy. The values of these parameters are calculated using the following relations.

$$\text{Mean susceptibility} \\ (K_m) = (K_1 + K_2 + K_3)/3 \quad (\text{ref. 14}), \quad (1)$$

$$\text{Magnetic lineation } (L) = K_1/K_2 \quad (\text{ref. 15}), \quad (2)$$

$$\text{Magnetic foliation } (F) = K_2/K_3 \quad (\text{ref. 16}), \quad (3)$$

$$\text{Degree of anisotropy } (D) = K_1/K_3 \quad (\text{ref. 14}), \quad (4)$$

$$\text{Eccentricity } (E) = K_2^2 / K_1 K_3 \quad (\text{refs 17, 18}), \quad (5)$$

$$\text{Corrected degree of anisotropy } (P_j) = \exp \{2[(n_1 - n_m)^2 \\ + (n_2 - n_m)^2 + (n_3 - n_m)^2]\}^{1/2} \quad (\text{ref. 19}), \quad (6)$$

$$\text{Shape parameter } (T_j) = (2n_2 - n_1 - n_3)/(n_1 - n_3); \\ \text{where } n_i = \log K_i \quad (\text{ref. 20}). \quad (7)$$

The shape of AMS ellipsoids can be calculated using the Flinn diagram<sup>21</sup>, which is a plot of  $F$  versus  $L$ , and, Jelinek plot<sup>19</sup> where the  $P_j$  value is plotted against the  $T_j$  value. However, the corrected degree of anisotropy and shape parameter are more intrinsic properties and thus the Jelinek plot yields more precise results. Hence, the latter is used for ellipsoid shape determination in the present study.

Magnetic susceptibility and AMS were measured using a Bartington Susceptibility Meter (MS-2) housed in the Geophysics Laboratory, Department of Geological Sciences, Jadavpur University, Kolkata (India). Parameter values mentioned in eqs (1)–(7) were obtained from the

AMS-BAR software operating synchronously with the susceptibility meter.

### Petrography, magneto-mineralogy and chemical analysis

#### Petrography

Petrography of the rock samples was studied under transmitted light microscope to decipher the textural characteristics of rocks in the studied area. The dominant rock types present within the area are granite gneiss, amphibolites, quartzites and pegmatites. The textural characteristics of rocks were studied mainly to bring out the relationship of opaque minerals with that of the silicate ones.

Granite gneiss with alternating bands of dark and light-coloured minerals mainly consists of quartz, alkali feldspar, plagioclase and muscovite as the dominant felsic minerals and biotite, hornblende and titanomagnetite among the mafic minerals. At places, the typical feature of the granoblastic texture is present, showing the triple junction point defined by the amphibole, and the opaque grains (Figure 3 a). The amphibole grains are at places altered to biotite. The amphibolites are generally found to occur as patches within granite gneisses. The contacts of granite gneisses, with that of the amphibolite patches are ubiquitously sharp. The amphibolites consist dominantly of hornblende, plagioclase and minor quartz. Quartzites comprise mainly of quartz and opaque minerals with minor amount of chlorite and biotite. Veins of opaque (mainly titanomagnetite) are found to invade the quartzites (Figure 3 d). Effects of shearing are found within quartzites depicted by the presence of recrystallized and polygonal quartz grains (Figure 3 b). Pegmatites within the studied area are found to be intruded within the granite gneiss and are dominantly composed of alkali feldspar, quartz and muscovite.



Petrographic studies revealed that the opaque minerals (i.e. the magnetic minerals which contribute towards the magnetic susceptibility of the rocks (here titanomagnetite)) within the rocks show the following modes of occurrence. Within quartzites, the titanomagnetites are present as disseminated veins among recrystallized quartz grains and sometimes the veins also include quartz grains or parts of them (Figure 3 *d*). Some magnetite grains show anastomosing fractures (Figure 3 *g*). Opaque minerals (mainly magnetite) are also found to occur as chadacrysts within the host silicate oikocryst (Figure 3 *b*).

Apart from the above mentioned primary opaques, some secondary opaques/magnetic minerals are found to develop along the grain boundaries of silicate grains (Figure 3 *h*).

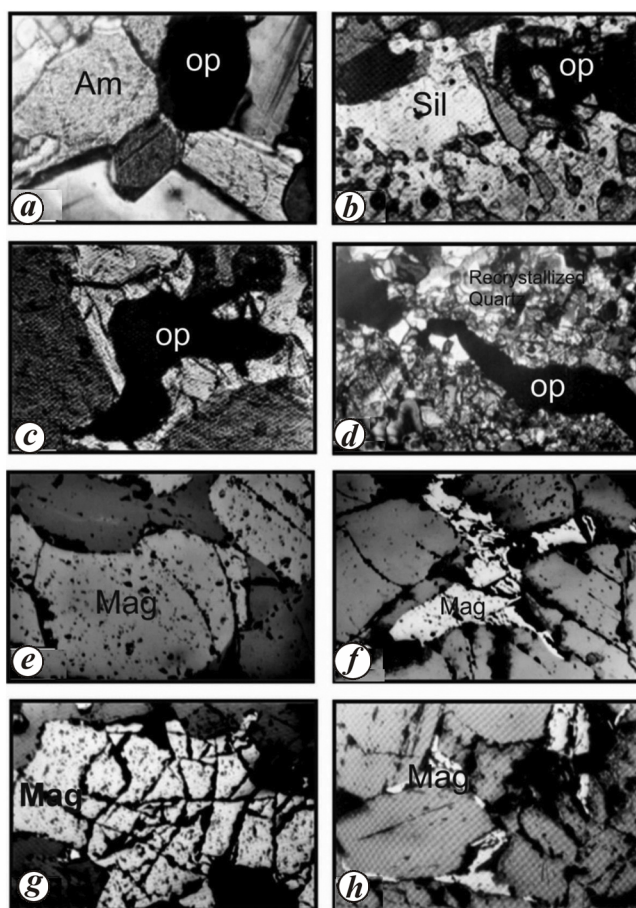


**Figure 3.** *a*, Granoblastic texture with polygonal mosaic defined by the amphibole and opaque grains (TL); *b*, Opaque grains present as inclusions within the silicates (TL); *c*, Opaque grains present as micro-folded grain with thicker hinge and thinner limbs (TL); *d*, Recrystallized quartz grains within quartzite with vein of opaque through it (TL); *e*, Stage-2 of low temperature primary oxidation of titanomagnetite (RL); *f*, Stage-3 of low temperature primary oxidation in titanomagnetite (RL); *g*, Stage-4 of low temperature primary oxidation in titanomagnetite (RL); *h*, secondary grains of titanomagnetite oxidized along the grain boundaries of the silicates (RL). TL, Transmitted light; RL, Reflected light.

### Magneto-mineralogy

A study under reflected light showed that titanomagnetite is the dominant Fe–Ti oxides within the studied sections. ‘Oxidation-exsolution’ is a phenomenon, due to which, laths and lamellae of ilmenite exsolve within the host magnetite grain. Oxidation of the magnetic minerals can occur both at high and low temperatures depending on the geological event experienced by the host rock. For example, rocks that undergo high temperature metamorphism contain magnetic minerals with effects of high temperature oxidation. The high temperature oxidation states of the Fe–Ti oxides were classified by Haggerty<sup>22</sup>. However in the present study, no traces of high temperature oxidation were seen within the studied samples. Chatterjee *et al.*<sup>23</sup> carried out similar magneto-mineralogical studies in the Eastern Ghats granulite belt where it was found that when rocks are metamorphosed to granulite facies, they have the magnetic minerals within oxidized state in high temperature. However, here the rocks are metamorphosed to amphibolite facies and thus high temperature oxidation stages are not encountered. Johnson and Hall<sup>24</sup> classified low temperature oxidation states of Fe–Ti oxides into five stages (stages 1–5) based on the nature of cracks which are their characteristic feature. They termed the cracks as ‘shrinkage cracks’, because these cracks develop due to cation deficiency resulting from the migration of Fe<sup>3+</sup> ions out of the titanomagnetite-spinel<sup>25,26</sup>. Development of microscopic to sub-microscopic cracks at the periphery of the grain occurs when low temperature oxidation initiates, signifying the occurrence of stage-2 (Figure 3 *e*). Stage-3 (Figure 3 *f*) is reached when the degree of low temperature oxidation increases, and the cracks start migrating from the periphery towards the centre of grains with subsequent filling of cracks by silicates. With further increase in the degree of low temperature oxidation, a network of these cracks is formed which reveals stage-4 (Figure 3 *g*). With further increase in oxidation, a ‘drop-let’-like structure is formed with the relict titanomagnetite within it (stage-5) which is not observed in the studied sections.

### Chemical analysis using AAS

Powdered rock (200 mg) was taken from each sample and were kept in a beaker, with water sprinkled over the powder to avoid loss of the sample. Later, 10 cc of hydrofluoric acid and 5 cc of perchloric acid were added to the sample and the mixture heated to 50°C for 1 h and at 90°C for 2 h until white fumes were produced. After the required time for heating, the beaker was cooled to room temperature. Once the solution reached room temperature, hydrochloric acid solution was added to it in 1 : 1 proportion and the solution was filtered through a filter paper into a volumetric flask. Distilled water was added

**Table 1.** Database for determination of iron concentration from AAS study

Sample no.	Weight of the sample taken (g)	Mother solution concentration (1000 ml)	Concentration (100 ml)
P/B/1	0.201	15 mg	1.5 mg
P/B/2	0.2	18 mg	1.8 mg
P/B/3	0.2	23 mg	2.3 mg
P/B/4	0.2	21 mg	2.1 mg
P/B/5	0.2	27 mg	2.7 mg
P/B/6	0.2	29 mg	2.9 mg
P/B/7	0.201	28 mg	2.8 mg
P/B/8	0.202	28 mg	2.8 mg
P/B/9	0.201	34 mg	3.4 mg
P/B/10	0.202	43 mg	4.3 mg
P/B/11	0.201	32 mg	3.2 mg
P/B/12	0.2	29 mg	2.9 mg
P/B/13	0.2	25 mg	2.5 mg

to the solution until the volume of the solution reached 100 ml. This solution is called the mother solution.

From the mother solution, daughter solution was prepared which was 10 times more dilute than the mother solution. These solutions were analysed in AAS.

The machine works on the principle that atoms of the target element absorb the light of resonant wavelength which passes through the cloud of atoms of the target element. The source of light remains different for different target elements, and in this case as Fe was the target element, oxy-acetelene flame was used as the source of light. Basically, when the light passes through the compounds, it supplies thermal energy to the latter and thus free atoms are released, which forms a cloud. These clouds of atoms actually absorb the light, and the proportion of light is a measure of that particular element in the sample. In the present study, both mother and daughter solutions were subjected to AAS analysis and the results obtained are provided in Table 1.

### AMS studies

The values of magnetic susceptibility show two dominant ranges represented by samples from the Paharpur and Gopalpur areas and Dangra nala–Dwarkeshwar river section area. Samples from the Paharpur and Gopalpur area have their values of susceptibility ranging between  $21.811 \times 10^{-2}$  and  $34.95 \times 10^{-2}$  SI units whereas in the Dangra nala–Dwarkeshwar river section, the values of susceptibility range from  $18.68 \times 10^{-2}$  to  $304.15 \times 10^{-2}$  SI units.

AMS studies were carried out to determine the nature and attitude of magnetic fabric elements and the values of the related AMS parameters. The parameters related to AMS were obtained from the combined operation of the Bartington Susceptibility Meter (MS-2) and AMS-BAR software. The values of mean susceptibility, magnetic lineation ( $L$ ), magnetic foliation ( $F$ ), degree of anisotropy and eccentricity ( $E$ ) were obtained (Table 2). The values

of  $F$  range from 1.1 to 1.4 and  $L$  range from 1 to 1.2. The degree of anisotropy ( $P_j$ ) lies between 1.127 and 1.387. The shape parameter ( $T_j$ ) is positive in maximum number of samples with few samples showing negative values. The values of  $T_j$  range between  $-0.904$  and  $0.904$ . The plot of  $P_j-T_j$  (ref. 19), also supports the fact that the shape of susceptibility ellipsoids is oblate (Figure 4). In the present study, it is seen that the plots are mainly within the  $F$  dominated field, i.e. the AMS ellipsoid shows oblate (or disc shaped) nature. The value of  $E$ , which is greater than 1, also corroborates the contention. On the other hand, the  $K_m-P_j$  plots (Figure 5) for the samples describe a dense cluster (cluster-1) and a rarer cluster (cluster-2). The  $P_j$  values are ubiquitously greater than 1.05 signifying higher degrees of anisotropy both in granite gneissic basement rocks and intrusive pegmatites. Cluster-2 is basically due to samples of gneisses which have higher concentration of ferro-magnetic minerals in them.

The  $K_1$ ,  $K_2$  and  $K_3$  axes were plotted on an equal area net. The minimum ( $K_3$ ) susceptibility axis remained concentrated to the centre whereas the maximum ( $K_1$ ) and intermediate ( $K_2$ ) susceptibility axes showed variation about the periphery which points to almost horizontal magnetic foliations in the studied rocks. The rose diagram for the  $K_1$  susceptibility axis defines similar trends (Figure 6). The  $K_1$  azimuths are in all four quadrants with varying intensity (Figure 6).

### Results and discussion

Primarily, the rocks of the studied area are of two types: metasedimentary and metabasics. The rocks are metamorphosed to amphibolite facies. All these rocks contain varying abundance of magnetic minerals with a wide range of textural relationships with silicate minerals. Studies under reflected-light depicted the presence of only low temperature oxidation stages of the titanomagnetites (Figure 3). Apart from the primary low temperature oxidation stages there are evidences of some

**Table 2.** Results from AMS measurements of the studied samples

Sample no./rock type	No. of cores	$K_m$	$F$	$L$	$D$	$K_1(D^0/I^0)$	$K_2(D^0/I^0)$	$K_3(D^0/I^0)$	$P_j$	$T_j$
PB-1a (GGP)	6	45.3	1.1	1.1	1.1	28.8/3.2	118.8/1.2	228.8/86.6	1.162	0.592
PB-4c (GGP)	6	111.6	1.1	1.0	1.2	10.9/3.1	109.5/69	111.8/74.2	1.197	0.840
PB-5b (GGP)	5	1394.1	1.1	1.1	1.1	338/3.3	68.7/4.7	205.6/85.2	1.244	0.409
PB-6a (GGP)	6	46.1	1.1	1.0	1.1	28.3/3.1	114.9/12	338.7/77.2	1.182	0.447
PB-10b (GGD)	6	111.4	1.1	1.1	1.2	10.3/3.2	109/69.1	114.3/78.0	1.387	0.724
PB-11b (GGD)	5	78.3	1.3	1.2	1.1	123.8/4.3	35.0/2.9	231.3/81.1	1.133	0.782
PB-12b (GGD)	6	68.9	1.3	1.2	1.2	122.3/2.5	33.0/1.4	235.5/85.5	1.192	0.432
PB-13c (GGD)	6	58.9	1.1	1.1	1.1	119.8/2.3	32.0/1.9	237.3/85.1	1.143	0.602
PB-19a (GGD)	7	95.6	1.4	1.0	1.4	216.3/2.3	306/10.8	114.5/79.0	1.127	0.595
PB-6d (PG)	8	83.2	1.1	1.0	1.1	246.9/3.6	144.2/14	356.3/85.2	1.202	-0.714
PB-14b (PG)	5	67.8	1.3	1.0	1.3	230.7/4.0	140.2/1.9	356.3/79.1	1.166	-0.391
PB-15d (PG)	6	57.8	1.3	1.0	1.0	119.9/2.3	29.1/4.4	227.5/86.3	1.149	-0.766
PB-16b (PG)	7	95.3	1.3	1.1	1.2	215.1/2.5	305/11.9	236.1/84.2	1.66	-0.432
PB-17a (PG)	6	1398.3	1.3	1.1	1.3	337.9/5.4	47.5/11.4	11.1/74.4	1.373	-0.199
PB-18c (PG)	7	83.2	1.4	1.0	1.1	310.5/8.5	51.8/1.3	205.3/85.2	1.576	-0.706

GGP, Granite gneiss (Paharpur and Gopalpur regions); GGD, Granite gneiss (Darkeshwar and Dangra Nala); PG, Pegmatite bodies.

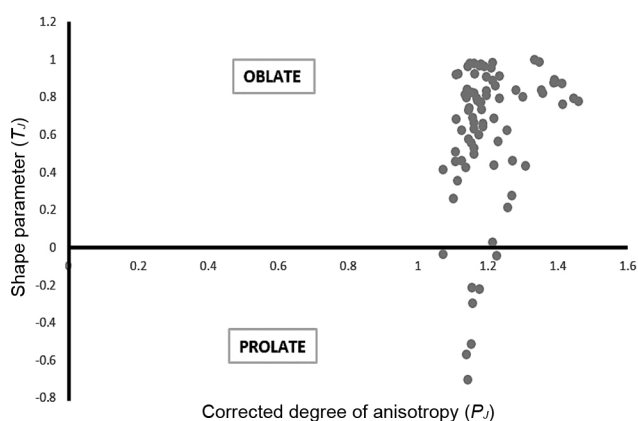


**Figure 4.** Jelinek plot ( $P_j$  versus  $T_j$  plot) for the samples studied showing overall oblate nature of the AMS ellipsoids.

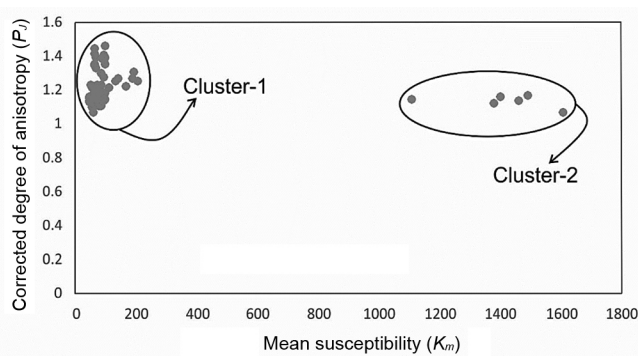


**Figure 5.**  $K_m$  versus  $P_j$  plots for the samples of the studied area.

secondary magnetic minerals developed along the grain boundaries of the silicates (Figure 3). Thus, there are two dominant states of oxidation of the magnetic minerals: primary low temperature oxidations and secondary oxidations. In Chatterjee *et al.*<sup>23</sup>, it is stated that the temperature-dependent oxidation of titanomagnetites cor-

responds to the attainment of peak metamorphic grade. Here the studied rocks belong to amphibolite facies which occur at a temperature range varying from 450°C to 750°C, occur much higher than 350°C, the temperature required for low temperature oxidation<sup>22</sup>. Thus, while attaining the peak metamorphic condition, the titanomagnetites underwent low temperature oxidation thereby developing corresponding features<sup>22</sup>. The secondary magnetic minerals present within the grain boundaries developed due to secondary processes which succeeded the attainment of the peak metamorphic condition. Such a post-peak metamorphic event may be pointed towards tectonic exhumation of deep-seated rocks towards the surface which caused the rocks to attain a domain of lower temperature and pressure, during which the secondary ultrafine grains of magnetite/titanomagnetite developed along the grain boundaries of the silicates.

From the chemical analysis of rocks using AAS, it is seen that the average concentration of iron within the rocks under study is 13.5%.

The mass susceptibility values of studied rocks, although very low, show two peak values which can be attributed to higher susceptibilities of the metabasics from the Paharpur and Gopalpur regions and granite gneisses from Dangra nala and Dwarakeshwar. However, from the  $K_m$ - $P_j$  plots it is seen that there exists no positive correlation between mean susceptibilities and corrected degrees of anisotropy. This proves that the magnetic anisotropy and magnetic fabrics are not controlled by bulk susceptibilities of the magnetic (ferro-, para- or dia-magnetic) minerals; rather they are controlled by deformation and tectonic features.

From the equal area plots, it is seen that the minimum susceptibility axis (poles to magnetic foliation) represents a strong cluster at the centre (Figure 6). This feature proves that magnetic foliation is near horizontal. This type of near-horizontal magnetic foliation is indicative of

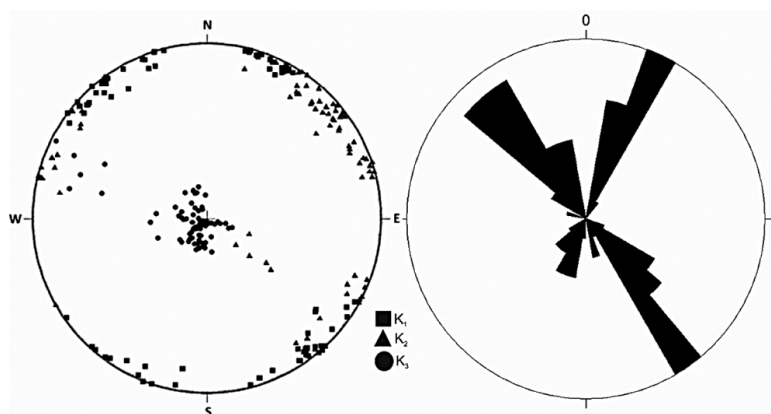


**Figure 6.** Plots on equal area net showing the distribution of the maximum, minimum and the intermediate susceptibility axes (left); Rose diagram for the  $K_1$  susceptibility axes showing the dominant trends (right).

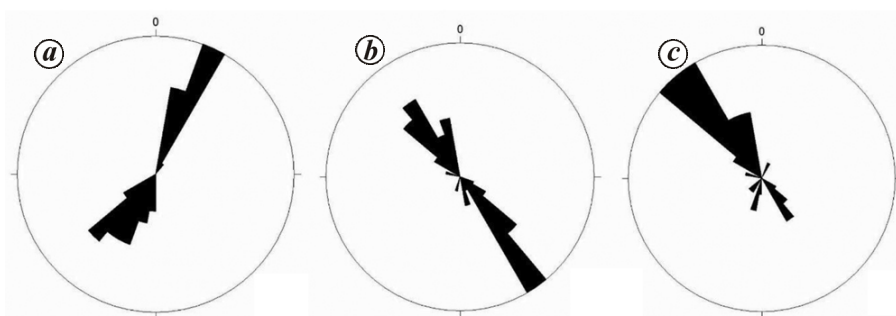


**Figure 7.** Rose diagrams representing the trends of  $K_1$  susceptibility axes from different sections of studied area. *a*, Granite gneiss of Paharpur and Gopalpur regions; *b*, Granite gneiss of Darkeshwar and Dangra nala area; *c*, Pegmatitic bodies.

the presence of isoclinal folds within the field<sup>2,4</sup>. Possibilities of near-horizontal magnetic foliation can also result from the presence of homoclinal planar structures. But in the present case such possibilities can be ruled out based on field evidences which suggests that the mesoscopic field foliation (gneissic banding) is not horizontal. Besides, studies by Baidya<sup>2</sup> and Mandal *et al.*<sup>4</sup> provide reports of the presence of migmatites near the studied rocks of Paharpur and Gopalpur region, which is also reflected in the distribution of susceptibility axes on the equal area diagram. Such inferences can be drawn in analogy with results obtained by Ferre *et al.*<sup>27</sup> from the Minnesota River Valley Complex in the Superior province of Canadian Shield.

Further, it is seen that the foliation trend of metabasic rocks in the Paharpur and Gopalpur regions is NE–SW to NNE–SSW. Again, the foliation trend of the granite gneisses in the Dangra nala and the Dwarakeshwar river section is NW–SE. The elongated coarse crystals in the pegmatitic intrusive bodies also have similar trends of NW–SE. The rose diagram of maximum susceptibility vectors (Figure 6), describes three major petals in NE, SE and NW directions. The NE–SW trend is a clear replica-

tion of the trends of gneissic foliation mineral lineation in Paharpur and Gopalpur region (Figure 7 *a*). The NW–SE trend of the petals is an offspring of two mesoscopic fabrics: gneissic foliation in Darkeshwar and Dangra nala areas (Figure 7 *b*) and mineral lineation in the pegmatites (Figure 7 *c*). Thus, the bimodal magnetic fabric trends observed can be attributed to two major geological events in the area: first, the deformation vis-à-vis metamorphism and consequent development of gneissic foliation, and, secondly, emplacement trend of the pegmatitic veins.

The girdles of the  $K_1$  axes generally indicate the direction, perpendicular to the direction of maximum shortening<sup>28–30</sup>. This helps to reach a conclusion that the  $K_1$  axis is parallel to the direction of maximum elongation in a deformation event. Now, the magnetic foliation in the gneisses in Paharpur and Gopalpur region is NE–SW to NNE–SSW and that of Darkeshwar and Dangra nala region is NW–SE. Thus, the  $K_1$  trend for the deformed basement gneisses (which can be considered as the direction of maximum elongation during deformation) is variable over the studied area which points to the signatures of at least two deformational events in magnetic fabrics. In the case of pegmatites, the  $K_1$  trends NW–SE, which

has close accordance with the mineral lineation developed in the pegmatitic bodies by elongated grains. Thus, the magnetic fabrics draw a close analogy with the pegmatite intrusion and the deformation patterns in Darkeshwar and Dangra nala area.

The susceptibility ellipsoids are dominantly oblate shaped; yet some lie within the prolate field (Figure 4). Hrouda and Janak<sup>31</sup> suggested that the change of shape of the ellipsoid occurs from oblate to prolate and with further increase in the intensity of deformation, the shape further changes to oblate on account of increased accumulation of flattening strain during deformation. However, the presence of both oblate and prolate-shaped ellipsoids in this particular area stands quite different. From the nature of susceptibility ellipsoids in the studied area, it can be firmly stated that deformation of rocks in the area occurred due to flattening strain which led to the development of a foliation dominated fabric in the area. This contention is further corroborated by the greater value of  $F$  than  $L$  obtained from the susceptibility data (Table 2). However, the plots lying within the prolate field need explanation. Pegmatites are coarse-grained magmatic rocks which do not possess any primary elongated grains and can have their susceptibility axes aligned to the flow direction leading to the development of a flow parallel linear fabric. However, field evidences suggest that pegmatitic bodies possess mineral lineation with a trend of NW–SW, plunging moderately towards NW, which is similar to  $K_1$  trends in pegmatites and also in the gneisses of Darkeshwar and Dangra nala areas. This parity in patterns of both mesoscopic and magnetic foliation proves that the emplacement of pegmatite bodies was synchronous with the deformation recorded by the fabrics of Darkeshwar and Dangra nala.

## Conclusions

From mineralogical studies, it is clear that the dominant magnetic mineral present within the studied rock is titanomagnetite which is ferro-magnetic. Still it shows very low values of susceptibility which is on account of lower concentration of ferro-magnetic minerals. Also, the paramagnetic susceptibilities of mica minerals and diamagnetic susceptibility of quartz can contribute towards the overall decrease in the magnetic susceptibility values. The presence of ultrafine grains of secondary magnetite, which occur as droplets along silicate grain boundaries is indicative of upliftment of the Earth's crust with slow cooling<sup>32</sup>. During upliftment and/or exhumation of deep crustal rocks there occurs release of pressure which leads to the development of cracks within the oxide minerals which further gets filled in by silicates. Thus these features can be attributed towards upliftment of crust and slow cooling followed by cation migration. The AMS results from the study are significant in correlating the

basement deformation and intrusion of pegmatite bodies. First, it is to be noted that the maximum stretching direction as determined from the trend of  $K_1$  axis is bimodal, NNE–SSW and NW–SE. This proves that there were at least two events of deformation suffered by the gneissic basement. The pegmatite bodies from the field evidences are found to emplace much later but display a trend of  $K_1$  like that of the gneissic basement at Darkeshwar and Dangra nala areas. Thus, the pegmatite bodies were intruded where the region experienced an elongation in NW–SE direction which explains the mineral lineation observed in the pegmatites and the trends of  $K_1$  in the same. Such linear features developed in pegmatite veins are also supported by the prolate nature of ellipsoids from pegmatite samples. Thus, it can be concluded that the deformation events were the driving forces which developed the magnetic fabric. Also, magnetic anisotropy is not due to ferromagnetic susceptibility of the titanomagnetite but due to dia-magnetic and para-magnetic susceptibilities of silicates.

1. Watson, J. V., Vertical movements in Proterozoic structural provinces. *Philos. Trans. R. Soc. London A*, 1976, **280**.
2. Baidya, T. K., Archean metallogeny and crustal evolution in the East Indian shield. *Earth Sci. (Special Issue: Archean Metallogeny and Crustal Evolution)*, 2015, **4/4-1**, 1–14.
3. Ghose, N. C., Geology, tectonics and evolution of the Chhotanagpur granite-gneiss complex, Eastern India. In *Recent Researches in Geology*, Hindustan Pub. (Delhi), 1983, vol. 10, pp. 211–247.
4. Mandal, A., Ray, A., Debnath, M. and Paul, S. P., Petrology, geochemistry of hornblende gabbro and associated dolerite dyke of Paharpur, Puruliya, West Bengal: Implication for petrogenetic process and tectonic setting. *J. Earth Syst. Sci.*, 2012, **121**(3), 793–812.
5. Baidya, T. K., Chakravarty, P. S., Drubetskoy, E. and Khiltova, V. J., New geochronological data on some granitic phases of the Chhotanagpur granite gneiss complex in the northwestern Purulia district, West Bengal. *Indian J. Earth Sci.*, 1987, **14**(2), 136–141.
6. Baidya, T. K., Maity, N. and Biswas, P., Tectonic phases and crustal evolution in a part of the Eastern Chhotanagpur Gneissic Complex. *J. Geol. Soc. India*, 1987, **34**(3), 318–324.
7. Sengupta, D. K. and Sarkar, S. N., Structure of the granitic rock and associated metamorphites of the area around Muri-Silli-Jhalida, Ranchi and Purulia Districts, India. In 22nd International Geological Congress, 1964, vol. 4, pp. 374–389.
8. Ghosh, N. C., Geology, tectonic evolution of the Chhotanagpur granite gneiss complex, eastern India. *Recent Res. Geol.*, 1983, **10**, 211–247.
9. Mazumder, S. K., Crustal evolution of Chhotanagpur gneissic complex and the Mica Belt of Bihar. In Precambrian of the Eastern Indian Shield. Geological Society of India Memoir, 1988, vol. 8, pp. 49–83.
10. Sarkar, A. N., Tectonic evolution of the Chhotanagpur plateau and Gondwana basins in eastern India: An interpretation based on supra-subduction geological processes. In Precambrian of the Eastern Indian Shield. Geological Society of India Memoir, 1988, vol. 8, pp. 127–146.
11. Tarling, D. and Hrouda, F., *Magnetic Anisotropy of Rocks*, Springer, 1993, pp. 14–27.
12. Sen, K., Sharma, R. and Arora, B. R., Influence of magnetic fabric anisotropy on seismic wave velocity in paramagnetic granites



- from NW Himalaya: Results from preliminary investigations. *J. Geol. Soc. India*, 2010, **76/4**, 322–330.
13. Jayagondaperuma, R., Dubey, A. K. and Sen, K., Structural and magnetic fabric studies of recess structures in the western Himalaya: Implications for 1905 Kangra earthquake. *J. Geol. Soc. India*, 2010, **75/1**, 225–238.
  14. Nagata, T., Rock magnetism. In *Maruzen*, 1961, 2nd edn, p. 350.
  15. Blasley, J. R. and Buddington, A. F., Magnetic susceptibility anisotropy and fabric of some Adirondack granites and orthogenesis. *Am. J. Sci.*, 1960, **258/A**, 6–20.
  16. Stacey, F. D., Joplin, G. and Lindsay, J., Magnetic anisotropy and fabric of some foliated rocks from S.E. Australia. *Geophys. Pura Appl.*, 1960, **47**, 30–40.
  17. Hrouda, F., Chlupacova, M. and Rejl, L., The mimetic fabric of magnetite in some foliated granitoids, as indicated by magnetic anisotropy. *Earth Planet. Sci. Lett.*, 1971, **11**, 4–38.
  18. Hrouda, F., Janak, F., Rejl, L. and Weiss, J., The use of magnetic susceptibility anisotropy for estimating the ferromagnetic mineral fabrics of metamorphic rocks. *Geol. Rundsh.*, 1971, **60**, 42–1124.
  19. Jelenik, V., Characterization of the magnetic fabric of rocks. *Tectonophysics*, 1973, **79**, 7–63.
  20. Hrouda, F., Magnetic anisotropy of rocks and its application in Geology and Geophysics. *Geophys. Surveys*, 1982, **5**, 37–82.
  21. Flinn, D., On folding during three-dimensional progressive deformation. *Q. J. Geol. Soc. London*, 1962, **118**, 385–433.
  22. Haggerty, S. E., Opaque mineral oxides in terrestrial igneous rocks. In *Oxide Minerals* (ed. Rumble, D.), Mineral. Soc. Am., Short Course Notes, 3, Hg101–Hg300.
  23. Chatterjee, S., Gain, D. and Mondal, S., Magneto-mineralogy characterization and analysis of magnetic fabrics of the high-grade rocks from Chilka Lake area, Eastern Ghats belt, India. *Earth Sci. India*, 2016, **9/1**, 29–47.
  24. Johnson, H. P. and Hall, J. M., A detailed rock magnetic and opaque mineralogy study of the basalts from Nazca Plate. *Geophys. J. R. Astr. Soc.*, 1978, **52**, 45–64.
  25. Prevot, M., Remond, G. and Caye, R., Etude de la transformation d'untitano magnetite-en-titanomaghemite-dansunerochevolcanique. *Bull. Soc. Fr. Min. Cristallogr.*, 1968, **91**, 65.
  26. Akimoto, T., Kinoshita, H. and Furuta, T., Electron probe micro-analysis study on process of Low temperature oxidation of titanomagnetite. *Earth Planet. Sci. Lett.*, 1984, **71**, 263–278.
  27. Ferre, E. C., Martín-Hernández, F., Teyssier, C. and Jackson, M., Paramagnetic and ferromagnetic anisotropy of magnetic susceptibility in migmatites: measurements in high and low fields and kinematic implications. *Geophys. J. Int.*, 2004, **157**, 1119–1129.
  28. Rathore, J. S., Magnetic susceptibility anisotropy in the Cambrian slate belt of North Wales and correlation with strain. *Tectonophysics*, 1979, **53**, 83–97.
  29. Goldstein, A. G., Magnetic susceptibility anisotropy of mylonites from the Lake Char Mylonite Zone, SE New England. *Tectonophysics*, 1980, **66**, 197–211.
  30. Mondal, S., Piper, J. D. A., Hunt, L., Bandopadhyay, G. and BasuMallik, S., Palaeomagnetic and rock magnetic study of charnockites from Tamil Nadu, India, and the 'Ur' protocontinent in Early Palaeoproterozoic times. *J. Asian Earth Sci.*, 2009, **34**, 493–506.
  31. Hrouda, F. and Janak, F., The changes in shape of the magnetic susceptibility ellipsoid during progressive metamorphism and deformation. *Tectonophysics*, 1976, **4**, 135–148.
  32. Zhang, J. and Piper, J. D. A., Magnetic fabric and post-orogenic uplift and cooling magnetisations in a Precambrian granulite terrain: The Datong-Huai'an region of the North China Shield. *Tectonophysics*, 1994, **234**, 227–246.

ACKNOWLEDGEMENTS. We acknowledge laboratory facilities from the Department of Geological Sciences, Department of Metallurgy and Centre for Bioequivalence, Jadavpur University. P.R. and A.B. express their gratitude to Goutam Bandopadhyay and Bhaskar Bose for assistance during field work. We also thank Subrata Sardar and Gautom Munian (Geologists, GSI) for assistance in the preparation of the map. Discussions with Dipanjan Mazumdar (Asutosh College) proved fruitful during the revision of the manuscript. S.C. acknowledges Rimjhim Maity (Jadavpur University) for assisting in field map preparation during the review.

Received 12 December 2016; revised accepted 21 December 2017

doi: 10.18520/cs/v114/i09/1894-1902